Iodine Substituted Tetrathiafulvalene Radical Cation Salts with $[M(isoq)_2(NCS)_4]^-$ Anions where M = Cr^{III}, Ga^{III}: Role of I···S and S···S Contacts on Structural and Magnetic Properties

Katel Hervé,[†] Olivier Cador,[†] Stéphane Golhen,[†] Karine Costuas,[†] Jean-François Halet,[†] Takashi Shirahata,[‡] Tsuyoshi Muto,[‡] Tatsuro Imakubo,[‡] Akira Miyazaki,[§] and Lahcène Ouahab*,[†]

L.C.S.I.M., UMR 6511 CNRS, Institut de Chimie de Rennes, Université de Rennes 1, 35042 Rennes Cedex, France, Initiative Research Unit, RIKEN, 2-1 Hirosawa, Wako, Saitama 351-0198, Japan, and Department of Chemistry, Tokyo Institute of Technology, 2-12-1-W4-1 O-okayama, Meguro-ku, Tokyo 152-8551, Japan

Received October 4, 2005. Revised Manuscript Received November 28, 2005

The preparation, crystal structures, extended Hückel theory band structure, and density functional theory (DFT) calculations and conducting and magnetic properties of seven new charge-transfer salts, formulated as $(D)_2[M^{III}(isoq)_2(NCS)_4]$, where D = DIET (diiodo(ethylenedithio)tetrathiafulvalene), DIETS (diiodo-(ethylenedithio)diselenadithiafulvalene), M = Cr, Ga, and isoq = isoquinoline, are reported. For each donor two different phases called **a** and **b** were obtained. Crystal data for $(DIET)_2[Cr(isoq)_2(NCS)_4]$ (**1**) are as follows: phase **a**, triclinic $P\bar{1}$, a = 9.8645(6) Å, b = 10.3255(8) Å, c = 13.7712(8) Å, α = 87.905(5)°, β = 75.981(5)°, γ = 80.712(2)°; phase **b**, triclinic $P\bar{1}$, a = 10.6760(5) Å, b = 11.3000(6) Å, c = 11.3930(9) Å, α = 101.256(2)°, β = 96.755(2)°, γ = 97.342(5)°. All compounds exhibit semiconductive behavior with room-temperature resistivity ranging from 2×10^3 to 5×10^4 Ω cm. Donors in the mixed-valence-state form dimers. They are connected to anions through very short I···S contacts (S2···I2 = 3.248(2) Å for **1a**). The magnetic measurements and spin density DFT calculations revealed that iodine atoms are good structural agents but are poor magnetic mediators to promote superexchange interactions between the donors and the inorganic anions. Our analyses reveal also that in these charge-transfer salts the magnetic interactions between spin carriers are mainly ensured by short intermolecular S···S contacts.

Introduction

The well-known TTF (tetrathiafulvalene) charge-transfer salts are still the subject of intense investigations.[1] Current activities in this field comprise development of multifunctional materials.[2] Interplay between magnetic properties of localized transition-metal d spins and mobile electrons of mixed-valence TTFs have been reported in several salts such as $(BEDT-TTF)_3[MnCr(C_2O_4)_3]$ (BEDT−TTF = bis(ethylenedithio)tetrathiafulvalene),[3] $(BETS)_2[FeCl_4]$ (BETS = bis(ethylenedithio)tetraselenafulvalene,[4] $(Cl-TET-TTF)_2[FeX_4]$ (X = Cl, Br; Cl−TET−TTF = 4,5-bis(methylthio)-4′,5′-ethylenedithiotetrathiafulvalene).[5] These compounds consist of discrete organic radical cations with inorganic anions containing paramagnetic transition metals. However, in this type of salt, through-space interactions between d and π electrons are very weak. To increase these interactions, several ideas are currently under investigation. These include the following: (i) The preparation of paramagnetic transition-metal coordination complexes where the paramagnetic center and the TTF are covalently linked.[2c] Hence, numerous functionalized TTFs have been prepared as well as their metal complexes.[6] (ii) The use of anions containing π and NCS^- ligands, which can enable both S···S and π···π interactions between the conducting and magnetic systems. Thus, materials presenting bulk ferrimagnetism in TTF- and TTP (tetrathiapentalene)-based salts with transition temperatures (T_C) ranging from 4.2 to 8.9 K[7,8] were obtained using isothiocyanato complexes $[M^{III}(NCS)_4(L)_n]^-$ where M = Cr and Fe and L = 1,10-phenanthroline (phen) or isoquinoline (isoq). (iii) A third strategy utilizes functionalized organic donors such as iodine substituted donors[9] combined with

* To whom correspondence should be addressed. E-mail: lahcene.ouahab@univ-rennes1.fr.
[†] Université de Rennes 1.
[‡] RIKEN.
[§] Tokyo Institute of Technology.

(1) (a) *Chem. Rev.* **2004**, *104* (11) and references therein. (b) Ishiguro, T.; Yamaji, K.; Saito, G. *Organic Superconductors*, 2nd ed.; Springer-Verlag: Heidelberg, Germany, 1998. (c) Williams, J. M.; Ferraro, J. R.; Thorn, R. J.; Carlson, K. D.; Geiser, U.; Wang, H. H.; Kini, A. M.; Whangbo, M. H. *Organic Superconductors. Synthesis, Structure, Properties and Theory*; Prentice Hall: Englewood Cliffs, NJ, 1992.
(2) (a) Graham, A. W.; Kurmoo, M.; Day, P. *J. Chem. Soc., Chem. Commun* **1995**, 2061. (b) Coronado, E.; Day, P. *Chem. Rev.* **2004**, *104*, 5419. (c) Ouahab, L.; Enoki, T. *Eur. J. Inorg. Chem.* **2004**, *5*, 933.
(3) Coronado, E.; Galan-Mascaros, J. R.; Gomez-García, C. J.; Laukhin, V. N. *Nature* **2000**, *408*, 447.
(4) Kobayashi, H.; HengBo, C.; Kobayashi, A. *Chem. Rev.* **2004**, *104*, 5265.
(5) Miyazaki, A.; Enoki, T. *Chem. Rev.* **2004**, *104*, 5449.
(6) (a) Iwahori, F.; Golhen, S.; Ouahab, L.; Carlier, R.; Sutter, J.-P. *Inorg. Chem.* **2001**, *40*, 6541. (b) Setifi, F.; Ouahab, L.; Golhen, S.; Yoshida, Y.; Saito, G. *Inorg. Chem.* **2003**, *42*, 1791. (c) Liu, S.-X.; Dolder, S.; Franz, P.; Neels, A.; Stoeckli-Evans, H.; Decurtins, S. *Inorg. Chem.* **2003**, *42*, 4801. (d) Arvarvari, N.; Fourmigué, M. *Chem. Commun.* **2004**, 1300.

10.1021/cm052199q CCC: $33.50
Published on Web 12/27/2005

paramagnetic anions containing π and CN^- ligands, which can enable both −I···N− and $\pi\cdots\pi$ interactions between the conducting and magnetic systems.[10] Here we propose a combination between points ii and iii, that is, assembly of iodine substituted donors and anions with π and NCS^- ligands. Hence, new charge-transfer salts are obtained, namely, $(D)_2[M(isoq)_2(NCS)_4]$, where D = DIET (diiodo-(ethylenedithio)tetrathiafulvalene), DIETS (diiodo(ethylene-dithio)diselenadithiafulvalene) and M = Cr^{III} and Ga^{III}. Their synthesis, X-ray crystal structures, and physical properties are reported. In these salts, donors are dimerized with one single electron per dimer. The stoichiometry is, therefore, one dimer per anion, or two donors for one $M(isoq)_2(NCS)_4$ moiety. Band structure and density functional theory (DFT) calculations have also been carried out.

Experimental Section

Synthesis. All experiments were conducted under argon, and the solvents were distilled. The starting materials DIET,[9d] DIETS,[9e] and $(isoqH)[Cr(isoq)_2(NCS)_4]$[7a] were prepared according to the literature procedure. All compounds were obtained by electrocrystallization, and the stoichiometries of each material were established by X-ray crystal structure analysis. For each donor, two different X-ray structures were obtained.

$(Bu_4N)[Ga(isoq)_2(NCS)_4]$. The synthesis is a two-step procedure. $(Bu_4N)_3[Ga(NCS)_6]_2$ is synthesized first, and then two NCS^- are exchanged with two isoq ligands. A mixture of three solutions made of 6.3 g of $(Bu_4N)[GaBr_4]$ in 50 mL of EtOH, 4.8 g of NaSCN in 50 mL of EtOH, and 7 g of $(Bu_4N)Br$ are refluxed for 3 h. After filtration at room temperature, to remove the NaBr salt, the solution is evaporated yielding 8.5 g of $(Bu_4N)_3[Ga(NCS)_6]_2$. A mixture of 5.0 g of $(Bu_4N)_3[Ga(NCS)_6]_2$ dissolved in 30 mL of EtOH and 1.1 g of isoq in 50 mL of EtOH is refluxed for 2 h and cooled to 5 °C. After standing for 3 days at this temperature, 1.9 g of $(Bu_4N)[Ga(isoq)_2(NCS)_4]$ is obtained by filtration as pink crystals.

$(D)_2[Cr(isoq)_2(NCS)_4]$ where D = DIET (1), DIETS (2). A mixture of black crystals as thick plates (phase **a**) and cubes (phase **b**) was obtained by anodic oxidation of 10 mg of donor D in a U-shape cell, with a constant current of 0.5 μA over 1 week. In each compartment, a solution of 40 mg of $(isoqH)[Cr(isoq)_2(NCS)_4]$ in 8 mL of freshly distilled dichloromethane was used as the electrolyte.

$(D)_2[Ga(isoq)_2(NCS)_4]$ where D = DIET (3), DIETS (4). Black crystals of **3** and **4** were obtained by a similar method: 10 mg of donor D, $I = 0.5$ μA, and 80 mg of $(Bu_4N)[Ga(isoq)_2(NCS)_4]$ in a mixture ethanol/dichloromethane (2:3; 16 mL). **3** crystallizes as two phases, **a** and **b**, while only phase **b** is obtained for **4**.

Table 1. Recapitulative of the Charge-Transfer Salts Based on Donors DIET and DIETS and the Anions $[M^{III}(isoq)_2(NCS)_4]$

anion	DIET	DIETS
$Cr(isoq)_2(NCS)_4$; $S = 3/2$	**1a**−**1b**	**2a**−**2b**
$Ga(isoq)_2(NCS)_4$; $S = 0$	**3a**−**3b**	**4b**

Table 1 summarizes the charge-transfer salts we have synthesized with the names of the donors, the names of the anions, which are paramagnetic for M = Cr^{III} and diamagnetic for M = Ga^{III}, the crystallographic phases, and finally the numbering that will be used hereafter.

X-ray. Single crystals of each compound were mounted on an Enraf-Nonius four circles diffractometer (CDFIX, Université de Rennes 1) equipped with a charge-coupled device camera and graphite monochromated Mo Kα radiation source ($\lambda = 0.710\ 73$ Å). Data collection was performed at room temperature. Effective absorption correction was performed (SCALEPACK).[11] Structures were solved with SHELXS-97[12] and refined with SHELXL-97[12] programs by the full matrix least-squares method, on F^2. Data collection parameters and crystallographic data for all compounds are summarized in Table 2.

Electronic Conductivity. Temperature dependences of the electronic conductivity were measured by a standard four-probe method using gold wire (10 or 18 mm diameter) and carbon paste.

Electronic Band Calculations. Intermolecular overlap integrals were calculated using highest occupied molecular orbitals of the donor molecules obtained from the extended Hückel theory with the use of semiempirical parameters[9d] for Slater-type atomic orbitals. Electronic band dispersions and Fermi surfaces were calculated using the intermolecular overlap integrals under the tight-binding approximation.[13]

Spin Density Calculations. Spin density was computed for the isolated cation and anion of **1b** with the aid of the DFT method, using the Amsterdam Density Functional (ADF) program,[14] developed by Baerends and co-workers.[15] Basis set IV was used to describe the atomic configurations. Representation of the spin density was done using MOLEKEL4.1.[16]

Magnetism. Magnetization was recorded with a Quantum Design MPMS SQUID magnetometer operating in the temperature range 2−300 K with a direct current magnetic field up to 5 T. χ_M stands for the molar magnetic susceptibility, and T is the temperature in kelvin. The experimental data were corrected from the diamagnetism of the sample holder, and the intrinsic diamagnetism of the materials was evaluated with Pascal's tables.

(7) (a) Turner, S. S.; Michaut, C.; Durot, S.; Day, P.; Gelbrich, T.; Hursthouse, M. B. *J. Chem. Soc., Dalton Trans.* **2000**, 905. (b) Turner, S. S.; Le Pevelen, D.; Day, P.; Prout, K. *J. Chem. Soc., Dalton Trans.* **2000**, 2739. (c) Setifi, F.; Golhen, S.; Ouahab, L.; Turner, S. S.; Day, P. *Cryst. Eng. Commun.* **2002**, *1*, 1. (d) Mas-Torrent, M.; Turner, S. S.; Wurst, K.; Vidal-Gancedo, J.; Ribas, X.; Veciana, J.; Day, P.; Rovira, C. *Inorg. Chem.* **2003**, *42*, 7544.

(8) (a) Setifi, F.; Golhen, S.; Ouahab, L.; Miyazaki, A.; Okabe, K.; Enoki, T.; Toita, T.; Yamada, J. *Inorg. Chem.* **2002**, *41*, 3786. (b) Miyazaki, A.; Okabe, K.; Enoki, T.; Setifi, F.; Golhen, S.; Ouahab, L.; Toita, T.; Yamada, J. *Synth. Met.* **2003**, *137*, 1195. (c) Setifi, F.; Ouahab, L.; Golhen, S.; Miyazaki, A.; Enoki, T.; Yamada; J. *C. R. Chim.* **2003**, *6*, 309.

(9) (a) Imakubo, T.; Sawa, H.; Kato, R. *J. Chem. Soc., Chem. Commun.* **1995**, 1667. (b) Imakubo, T.; Sawa, H.; Kato, R. *Mol. Cryst. Liq. Cryst.* **1996**, *285*, 27. (c) Imakubo, T.; Sawa, H.; Kato, R. *Synth. Met.* **1997**, *86*, 1883. (d) Imakubo, T.; Sawa, H.; Kato, R. *Synth. Met.* **1995**, *73*, 117. (e) Imakubo, T.; Tajima, N.; Tamura, M.; Kato, R. *J. Mater. Chem.* **2002**, *12*, 159.

(10) (a) Thoyon, D.; Okabe, K.; Imakubo, T.; Golhen, S.; Miyazaki, A.; Enoki, T.; Ouahab, L. *Mol. Cryst. Liq. Cryst.* **2002**, *376*, 25. (b) Ouahab, L.; Setifi, F.; Golhen, S.; Imakubo, T.; Lescouëzec, R.; Lloret, F.; Julve, M.; Świetlik, R. *C. R. Chim.* **2005**, *8*, 1286.

(11) Otwinowski, Z.; Minor, W. Processing of X-ray Diffraction Data Collected in Oscillation Mode. In *Methods in Enzymology: Macromolecular Crystallography*; Carter, C. W., Jr., Sweet, R. M., Eds.; Academic Press: New York, 1997; Vol. 276, part A, pp 307−326.

(12) Sheldrick, G. M. SHELX 97, Program for the Refinement of Crystal Structures, University of Göttingen: Göttingen, Germany, 1997.

(13) Mori, T.; Kobayashi, A.; Sasaki, Y.; Kobayashi, H.; Saito, G.; Inokuchi, H. *Bull. Chem. Soc. Jpn.* **1984**, *57*, 627.

(14) *ADF2004.01, Theoretical Chemistry*; Vrije Universiteit: Amsterdam, The Netherlands, SCM, 2003.

(15) (a) Baerends, E. J.; Ellis, D. E.; Ros, P. *Chem. Phys.* **1973**, *2*, 41. (b) te Velde, G.; Bickelhaupt, F. M.; Fonseca Guerra, C.; van Gisbergen, S. J. A.; Baerends, E. J.; Snijders, J. G.; Ziegler, T. *J. Comput. Chem.* **2001**, *22*, 931.

(16) *MOLEKEL 4.1*; Flükiger, P.; Lüthi, H. P.; Portmann, S.; Weber, J. Swiss Center for Scientific Computing (CSCS): Switzerland, 2000−2001.

Table 2. Crystal Data and Structure Refinements

	compound						
	1a	**2a**	**3a**	**1b**	**2b**	**3b**	**4b**
formula	$C_{38}H_{22}N_6S_{16}I_4Cr$	$C_{38}H_{22}N_6S_{12}I_4Se_4Cr$	$C_{38}H_{22}N_6S_{16}I_4Ga$	$C_{38}H_{22}N_6S_{16}I_4Cr$	$C_{38}H_{22}N_6S_{12}I_4Se_4Cr$	$C_{38}H_{22}N_6S_{16}I_4Ga$	$C_{38}H_{22}N_6S_{12}I_4Se_4Ga$
fw	1635.18	1822.78	1652.90	1635.18	1822.78	1652.90	1840.5
T, K	293	293	293	293	293	293	293
cryst syst	triclinic	triclinic	triclinic	triclinic	triclinic	triclinic	triclinic
space group	$P\bar{1}$	$P\bar{1}$	$P\bar{1}$	$P\bar{1}$	$P\bar{1}$	$P\bar{1}$	$P\bar{1}$
a, Å	9.8645(6)	9.9829(5)	9.8769(3)	10.6760(5)	10.7248(2)	10.6730(3)	10.7190(3)
b, Å	10.3255(8)	10.4011(5)	10.3545(3)	11.3000(6)	11.3782(3)	11.3330(3)	11.4100(3)
c, Å	13.7712(8)	13.7363(8)	13.7442(4)	11.3930(9)	11.4166(3)	11.4010(4)	11.4330(3)
α, deg	87.905(5)	88.374(2)	87.8389(12)	101.256(2)	100.975(1)	101.220(1)	100.894(1)
β, deg	75.981(5)	75.559(2)	76.1174(13)	96.755(2)	96.905(1)	96.719(1)	97.014(1)
γ, deg	80.712(2)	80.950(2)	80.4897(12)	97.342(5)	98.813(2)	97.577(1)	99.116(1)
V, Å^3	1343.05(15)	1363.94(12)	1345.81(7)	1322.51(14)	1335.41(6)	1326.35(7)	1338.98(6)
Z	1	1	1	1	1	1	1
ρ_{calcd}, g·cm^{-3}	2.022	2.219	2.039	2.053	2.267	2.069	2.282
μ, mm^{-1}	3.170	5.638	3.463	3.220	5.758	3.513	6.043
reflns collected	7166	8222	10 507	7547	12 335	10 802	11 346
unique reflns	4385	5027	6144	4586	7755	6054	6130
R_{int}	0.0372	0.0367	0.0193	0.0587	0.0313	0.0345	0.0210
final R_1[a]	0.0438	0.0472	0.0384	0.0489	0.0441	0.0514	0.0522
wR_2[b]	0.0921	0.1068	0.0959	0.1073	0.1088	0.1308	0.1448

[a] $R_1 = \sum||F_o| - |F_c||/\sum|F_o|$. [b] $wR_2 = \{\sum[w(F_o^2 - F_c^2)^2]/\sum[w(F_o^2)^2]\}^{1/2}$.

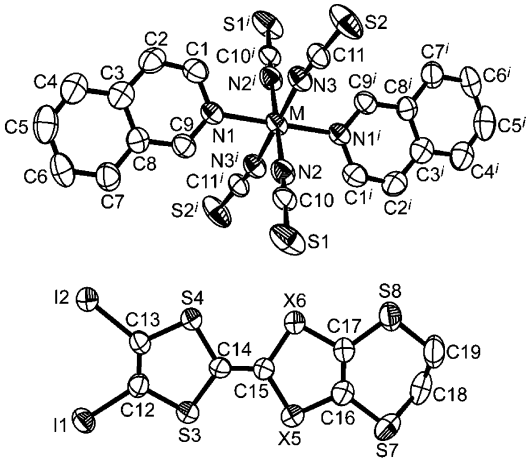

Figure 1. ORTEP drawing of **1a**. The same labeling scheme is used for all compounds. X = S, M = Cr for **1**; X = Se, M = Cr for **2**; X = S, M = Ga for **3**; and X = Se, M = Ga for **4**. *i*: $-x, -y, -z$.

Results and Discussion

Crystal Structure. An ORTEP drawing with 50% thermal ellipsoids of the donor and anion, with the atom numbering scheme, is shown in Figure 1 for compound **1a**. The labeling scheme is the same for all compounds.

*Phase **a**.* The asymmetric unit contains one donor molecule and one half $[M(isoq)_2(NCS)_4]^-$ anion lying on an inversion center in (0,0,0). All data are given here for **1a** and in brackets for **2a** and **3a**, respectively. The coordination sphere around the metal center is almost octahedral, where the four M−N (NCS) distances are slightly shorter (mean value 1.982 Å [1.986 and 2.005 Å]) than the M−N (isoq) separations: 2.073(5) Å [2.087(6) and 2.083(3) Å]. Selected bond distances are given in Table 3. The M−N−CS angles range from 170.5(6) to 173.3(6)° [from 172.6(7) to 173.3(7)° and from 168.8(4) to 171.9(4)°] and deviate slightly from linearity. The projection of the crystal packing in the *bc* plane is shown in Figure 2; it consists of alternating layers of organic and inorganic ions along the *c* axis. Anions are packed together thanks to $\pi-\pi$ interactions between adjacent isoq rings yielding anion chains along the *b* direction (distance between mean planes is equal to 3.533 Å [3.561 Å, 3.536 Å] and shortest distance is C3···C3 = 3.570(12) Å [3.636(13), 3.564(8) Å]).

Table 3. Selected Interatomic Distances in Phase a Compounds (in Å)

	1a	**2a**	**3a**
S3−C14	1.745(7)	1.748(7)	1.741(4)
S4−C14	1.754(7)	1.744(8)	1.742(4)
X5-C15	1.732(7)	1.861(7)	1.728(4)
X6-C15	1.728(7)	1.884(7)	1.739(4)
C15−C14	1.359(9)	1.364(10)	1.368(6)
M−N1	2.073(5)	2.087(6)	2.083(3)
M−N2	1.978(6)	1.983(7)	2.000(4)
M−N3	1.986(6)	1.989(6)	2.011(4)

In the organic layer, donors form dimerized chains along the *b* direction. The structural type is the so-called β'-type. The shortest intradimer X6···S3 bond is 3.645(3) Å [3.679(2) Å, 3.639 (2) Å]; the intradimer overlap is a ring-central C=C bond type (see Figure 3a). Neighboring dimers are shifted yielding only two S···S short contacts in the van der Waals (vdW) range (3.6 Å; see Figure 3b). The intradimer mean plane separation is equal to 3.497 Å [3.583 Å, 3.489 Å] while the interdimer one is 3.942 Å [4.019 Å, 3.953 Å]. Selected shortest intra- and interdimers S···S contacts are given in Table 4. Both shortest S···S intra and interdimer distances are in the vdW range. We can notice that the crystal structure is governed by two kinds of interactions between anions and donors. In the *bc* plane, there are two short contacts between iodine atoms of donors and sulfur atoms of anions which are remarkably shorter than the vdW distance (3.8 Å): S2···I2 = 3.248(2) Å [3.247(2) Å, 3.263(1) Å] and S1···I1 = 3.356(2) Å [3.371(2) Å, 3.341(1) Å] (see Figure 2). In the [$\bar{1}$11] direction, the stability of the structure is ensured by short contacts (shorter than the vdW distance) between sulfur atoms of the NCS groups of anions and donors. The shortest distance is X6···S1 = 3.4420(29) Å [3.3928(24) Å, 3.4425(18)

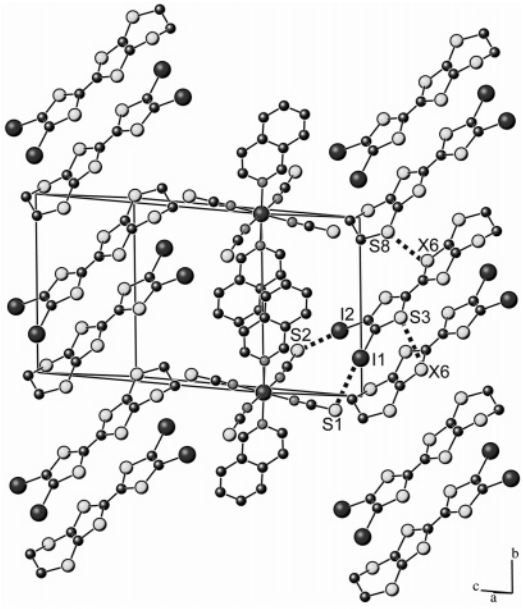

Figure 2. Crystal packing of **1a** (X = S) in the *bc* plane showing the alternating organic and inorganic layers.

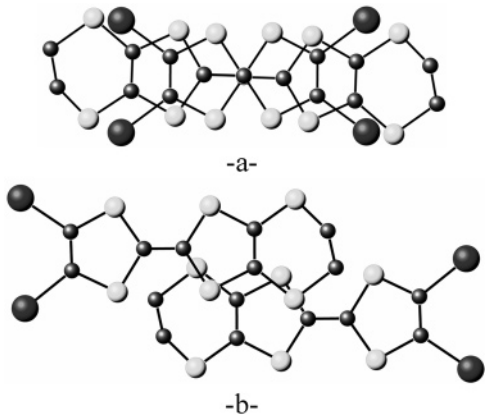

Figure 3. Intradimer (a) and interdimer (b) packing of **1a**.

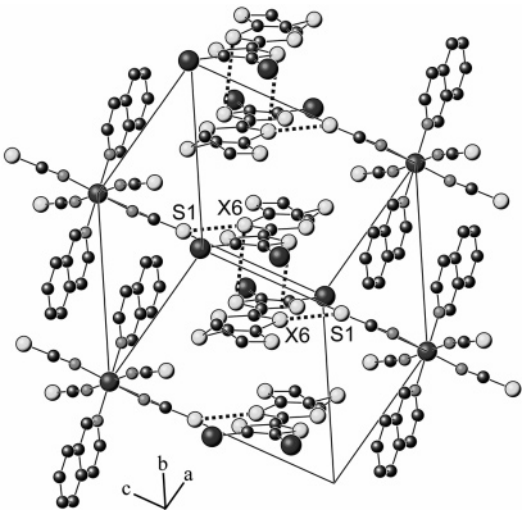

Figure 4. Crystal packing of **1a** showing the mixed organic−inorganic chains with the shortest anion−donor contacts (dashed lines).

Å]. These contacts generate mixed alternating organic−inorganic chains in the [$\bar{1}$11] direction (see Figure 4). We can notice that the mean plane calculated from four chalcogen atoms S3, S4, X5, and X6 and two carbon atoms C14 and C15 belonging to the central TTF-type skeleton forms an angle of 87.34(11)° [85.38(11)°, 87.14(6)°] with the mean plane calculated with all atoms of the isoq fragment.

Table 4. Selected Intermolecular Distances (in Å) and Angles (in deg) Observed between the TTF Skeleton Plane and the isoq Plane in the Asymmetric Unit

Phase **a**

	1a	**2a**	**3a**
S3−X6[a]	3.645(3)	3.679(2)	3.639(2)
S4−X5[a]	3.740(3)	3.776(2)	3.741(2)
X6−S8[b]	3.687(3)	3.772(2)	3.680(2)
S1[c]−I1	3.356(2)	3.371(2)	3.341(1)
S2−I2	3.248(2)	3.247(2)	3.263(1)
C3−C3[d]	3.570(12)	3.636(13)	3.564(8)
S1−X6[e]	3.4420(29)	3.3928(24)	3.4425(18)
angle	87.34(11)	85.38(11)	87.14(6)

Phase **b**

	1b	**2b**	**3b**	**4b**
S4-X5[f]	3.748(4)	3.748(1)	3.748(3)	3.755(2)
S3-X6[f]	3.727(4)	3.717(1)	3.729(3)	3.727(2)
S2−S3[g]	3.432(5)	3.436(2)	3.425(3)	3.434(3)
S1−I2[h]	3.475(3)	3.478(1)	3.488(2)	3.501(2)
S2−I1[i]	3.328(3)	3.329(1)	3.319(2)	3.316(2)
angle	16.46(13)	18.16(6)	17.29(9)	18.10(9)

[a] $-x-1, 1-y, -z-1$. [b] $-x-1, 2-y, -z-1$. [c] $-x, -y, -z$. [d] $-x, -1-y, -z$. [e] $-1-x, 1-y, -z$. [f] $-1-x, -1-y, 1-z$. [g] $-1-x, -1-y, -z$. [h] $-1-x, -y, 1-z$. [i] $x-1, y, 1+z$.

Table 5. Selected Interatomic Distances in Phase b Compounds (in Å)

	1b	**2b**	**3b**	**4b**
S3−C14	1.761(10)	1.740(5)	1.740(8)	1.738(8)
S4−C14	1.732(11)	1.742(5)	1.731(7)	1.744(7)
X5-C15	1.727(11)	1.881(5)	1.737(7)	1.878(7)
X6−C15	1.742(10)	1.891(4)	1.750(8)	1.882(8)
C15−C14	1.371(13)	1.370(6)	1.373(9)	1.360(10)
M−N1	2.090(8)	2.089(3)	2.081(5)	2.089(5)
M−N2	1.979(9)	1.989(4)	2.014(6)	2.009(6)
M−N3	1.975(10)	1.992(4)	2.001(6)	2.008(6)

*Phase **b***. The asymmetric unit contains one donor molecule and one half $[M(isoq)_2(NCS)_4]^-$ anion lying on an inversion center (0,0,0). All data are given here for **1b,** and we give the data for **2b**, **3b**, and **4b** in Table 5. The geometrical parameters of the $[M(isoq)_2(NCS)_4]^-$ anion are close to those observed in phase **a** with mean values for metal−N (NCS) distances and M−N (isoq) equal to 1.98(1) Å and 2.090(8) Å, respectively. The M−N−CS angles range from 167.0(9) to 174.2(9)°. The packing is different from phase **a** as donors do not form chains but pack as isolated centrosymmetric dimers.

The intradimer overlap is identical to that found in phase **a** with a ring−double bond overlap. The intradimer mean plane distance is equal to 3.604 Å. The shortest intradimer contacts are in the vdW range: X6···S3 = 3.727(4) Å (S···S = 3.6 Å, S···Se = 3.7 Å). Selected shortest intra- and interdimer S···S contacts are given in Table 4.

Along the *b* direction, the dimers are separated by the isoq ligands (see Figure 5a). As in phase **a**, the distances between iodine atoms of donors and sulfur atoms of anions, S2···I1 = 3.328(3) Å, are significantly shorter than the vdW distance. In this phase, the angle between the mean plane calculated from the six atoms belonging to the central TTF-type skeleton forms an angle of 16.46(13)° with the mean plane of the

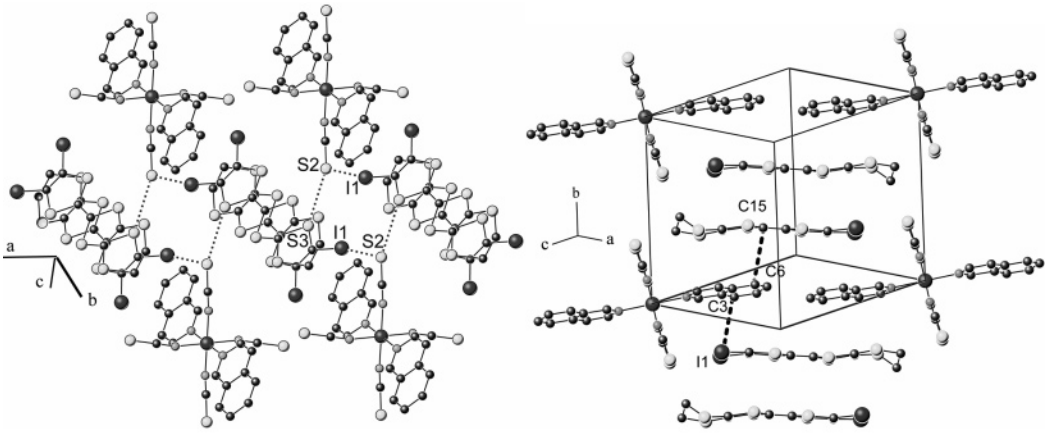

Figure 5. Crystal packing of **1b** along the *b* axis showing (a) the shortest intermolecular S···I contacts and (b) alternation of organic dimers and isoq rings and the shortest isoq···donor distances.

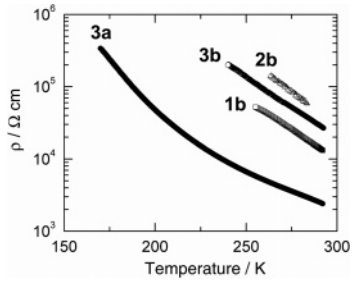

Figure 6. Temperature dependence of the resistivity for **1b**, **2b**, **3a**, and **3b**.

isoq fragment. The shortest interatomic distances between organic donors and isoq ligands, namely, C6···C15 = 3.501 Å on one side and C3···I1 = 3.705 Å on the other side, are longer than the sums of the vdW radii of the corresponding atoms (C···C = 3.1 Å and C···I = 3.65).

Conductivity. Figure 6 shows the temperature dependence of the resistivity for single crystals of **1b**, **2b**, **3a**, and **3b**. All salts are semiconducting with the room-temperature resistivity ranging from 2×10^3 to 5×10^4 Ω cm. Among the four salts, **3a** is less resistive. This is in agreement with the columnar arrangement of the donor molecules. Higher room-temperature resistivity of phase **b** (over 10^4 Ω cm) is in line with the isolated dimer structure.

Electronic Band Structure. Calculated intermolecular overlap integrals of the phase **a** salts is shown in Figure 7 and Table 6. The degree of the dimerization is larger than the usual TTF salts because of the large inclination of the donor molecules along the molecular long axis. The calculated overlap integrals are consistent with the strongly dimerized structure, and the intradimer overlap integrals *p* are 20−50 times larger than those of the interdimer overlap integrals, *q*, *r*, and *s*. Therefore, the shape of the Fermi surfaces is affected by the subtle balance of the interdimer quasi-one-dimensional overlap integrals. However, it does not reflect the intrinsic nature of the electronic band structures. Figure 8 shows the dispersions of the electronic bands. Their calculated bandwidths *W* are nearly 100 times smaller than those of the usual TTF-based organic conductors. It is due to the small absolute values of the interdimer overlaps, and it is the origin of the low conductivity of the

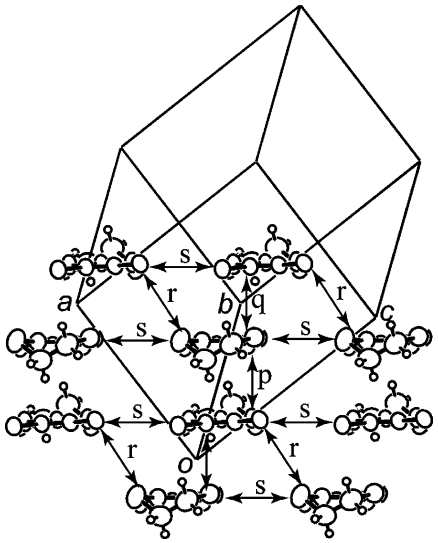

Figure 7. Molecular arrangement of the donor layer of the phase **a** salts.

Table 6. Calculated Overlap Integrals *S* (×10³) and Bandwidths *W* (eV) for the Phase a Crystals

	crystal				crystal		
	1a	**2a**	**3a**		**1a**	**2a**	**3a**
p	15.20	19.89	15.22	*s*	0.01	0.01	0.01
q	0.47	0.14	0.34	*W*	0.026	0.021	0.022
r	0.83	0.90	0.75				

phase **a** salts. Figure 9 and Table 7 show the overlap integrals of the phase **b** salts. The very small interdimer values (∼1/100 of intradimer) indicate that the donor dimers in the phase **b** crystals are almost isolated from a viewpoint of electronic band structure. An electron hopping conduction mechanism may be considered for the phase **b** salts.

Spin Density of Phase 1b. Spin dependent DFT calculations were carried out on the isolated inorganic anion $[Cr(isoq)_2(NCS)_4]^-$ and the organic dimer $(DIET)_2$ of phase **1b** to investigate the distribution of electronic spin within the system.

As shown in Table 8, the major part of the spin density in $[Cr(isoq)_2(NCS)_4]^-$ is localized on the chromium ion (2.80), in agreement with a formal Cr^{III} center. The rest of the positive spin density is mainly found on the sulfur atoms and to a lesser extent on the carbon atoms of the NCS groups

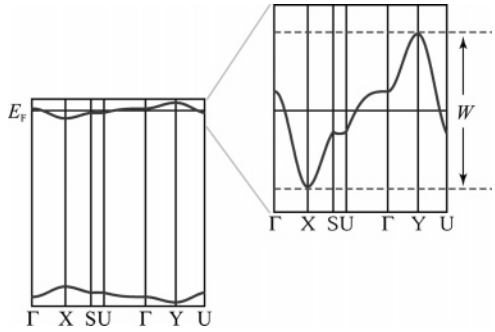

Figure 8. Calculated electronic band dispersions of the phase **a** salt. Entire view of the band structure (left) and the magnified view of the upper band structure (right).

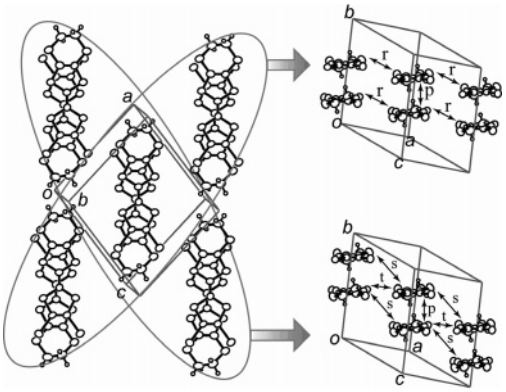

Figure 9. Molecular arrangement in the phase **b** crystals.

Table 7. Calculated Overlap Integrals *S* ($\times 10^3$) for the Phase b

	crystal					crystal			
	1b	**2b**	**3b**	**4b**		**1b**	**2b**	**3b**	**4b**
p	13.73	19.57	13.66	19.42	*s*	0.08	0.07	0.08	0.07
r	0.11	0.10	0.11	0.10	*t*	0.20	0.41	0.22	0.42

Table 8. Calculated Atomic Spin Densities for $[Cr(isoq)_2(NCS)_4]^-$ and $\{(DIET)_2\}^+$

$[Cr(isoq)_2(NCS)_4]^-$								
S1	S2	N1	N2	N3	C1	C10	C11	Cr
0.09	0.09	−0.06	−0.06	−0.05	0.02	0.03	0.03	2.80
$\{(DIET)_2\}^+$								
S4	S5	S6	S7	S8	C12	C13	C14	C16	C17
0.06	0.09	0.08	0.02	0.02	0.01	0.01	0.05	0.03	0.02

(see Figure 10). Very weak negative spin density is localized on the N atoms of the NCS and isoq ligands.

Spin population analysis of the donor $\{(DIET)_2\}^+$ indicates that the spin density is spread out mainly on the sulfur atoms and the central carbon atoms (see Table 8 and Figure 11). Interestingly enough, nearly no spin density (<0.004) is found on the terminal iodine atoms. Obviously, weak coupling between the inorganic and the organic moieties must occur via some interactions between sulfur and carbon atoms of the former and the latter.

Magnetism. For the structure of phase **b** salts being made of isolated dimers, we decided to discuss first the magnetic properties of compounds belonging to this phase.

*Phase **b**.* The $\chi_M T$ product of **3b** is temperature independent and is equal to 0.37 emu K mol^{-1}. This value corresponds to the spin-only value expected for one isolated radical with $s_{rad} = 1/2$. At room temperature, an ESR signal characteristic of organic radicals appears at $g = 2.011$.

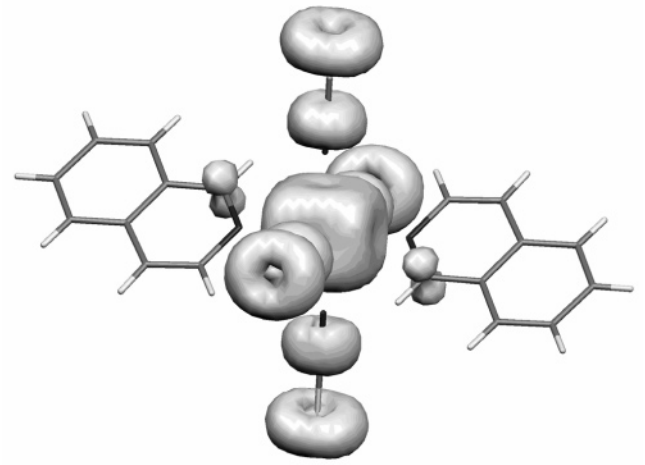

Figure 10. DFT-computed positive spin density of $[Cr(isoq)_2(NCS)_4]^-$ in **1b**. The isosurface plot is shown at 0.01 e/bohr^3.

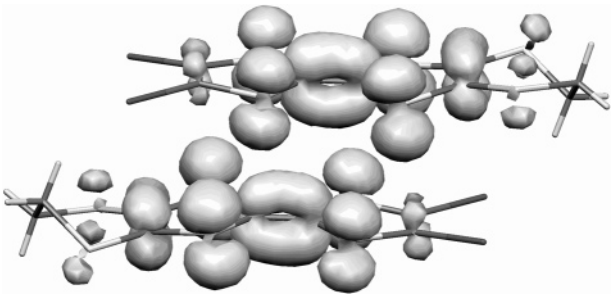

Figure 11. DFT-computed positive spin density of $\{(DIET)_2\}^+$ in **1b**. The isosurface plot is shown at 0.01 e/bohr^3.

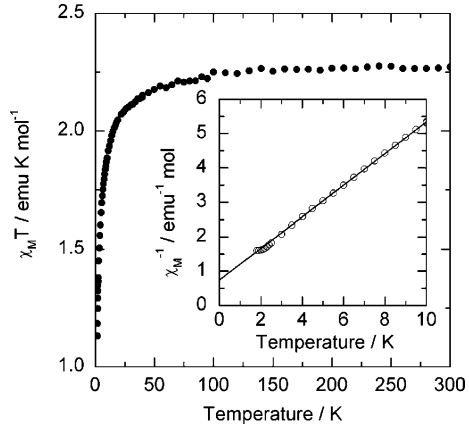

Figure 12. $\chi_M T$ vs T plot for **2b**. The inset shows the temperature dependence of χ_M^{-1} (points) with the best-fitted curve (see text).

According to the crystal structure there are no close contacts between dimers. The observed $\chi_M T$ value confirms that each donor dimer {D−D} carries one single electron. Indeed, two possible charge distributions on donors might be expected at the scale of material: (i) single dimers $\{D-D\}^{+\bullet}$ yielding to paramagnetic species and (ii) diamagnetic dimers $\{D^{\bullet}-D^{\bullet}\}^{2+}$ and $\{D-D\}^0$ in a 1:1 ratio ($\{D^{\bullet}-D^{\bullet}\}^{2+}$ being diamagnetic because of the very strong antiferromagnetic coupling between the two radicals).

The magnetic properties of **1b** and **2b** are very similar. At room temperature $\chi_M T$ for **2b** is equal to 2.27 emu K mol^{-1} (see Figure 12) which corresponds to the spin-only value expected for two uncoupled $s_{rad} = 1/2$ and $s_{Cr} = 3/2$ with $g = 2.00$. $\chi_M T$ is constant down to 100 K and then

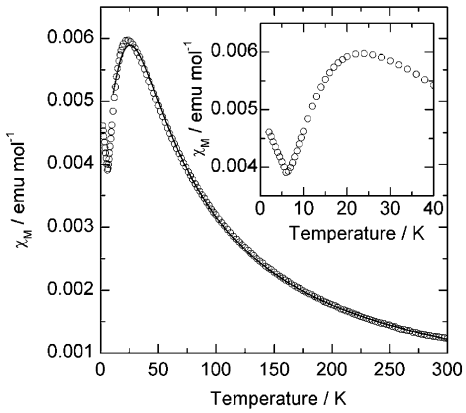

Figure 13. Temperature dependence of χ_M for **3a**. The solid line corresponds to the best adjusted curve (see text).

decreases. Finally, χ_M^{-1} passes through a minimum at $T = 1.9$ K. The magnetic susceptibility can be fitted with Curie−Weiss law $\chi_M = C/(T - \theta)$ (C is the Curie constant and θ is the Weiss temperature) in the temperature range 3.5−10 K with $C = 2.18$ emu K mol^{-1} and $\theta = -1.6$ K. Neither close contacts between anions nor $\pi-\pi$ overlap between isoq planes can be detected in phase **b**. However, there exists a short distance between two carbon atoms of adjacent isoq rings (C3···C3 = 3.262(20) Å), and one may suppose that superexchange interactions between Cr^{III} centers could take place through this contact. In one unit cell there are six short contacts between the donor at the center of the unit cell and the four anions at the corners, two S2···S3, two S2···I1, and two S1···I2, from which only S···S contacts contribute to the superexchange interactions. At the scale of the crystal these contacts define chains. In such spin topology, with antiferromagnetic interactions between adjacent spins, ferrimagnetic behavior would be anticipated. In other words, $\chi_M T$ would pass through a minimum while $\chi_M T$ would increase on lowering the temperature in the ferromagnetic case.[17] The value of θ is very small, and despite the short distances between spin carriers the amplitude of the interactions remains desperately small.

*Phase **a***. The magnetic properties of **3a** show more complex behavior than those of **3b**. The temperature dependence of χ_M of **3a** is represented in Figure 13. At room temperature $\chi_M T$ is equal to 0.37 emu K mol^{-1} which corresponds to the spin-only value for $s = 1/2$. χ_M increases on lowering the temperature, passes through a broad maximum at $T_{max} = 25$ K, and then decreases. Surprisingly, χ_M shows a minimum at $T_{min} = 6$ K. This minimum is perfectly reproducible, and the magnetization increases linearly with the magnetic field at 2 K which excludes the presence of paramagnetic impurities. In phase **a**, exchange type interaction between the spin of the dimers can take place because the shortest interdimer contact S6···S8 is in the vdW range. The magnetic system can be described by uniform chains of equally spaced spin 1/2. The spin Hamiltonian in zero field adapted to describe interactions between nearest neighbors is

$$H = -J\sum_{i=1}^{n-1} \mathbf{S}_i \cdot \mathbf{S}_{i+1}$$

with J being the exchange interaction parameter and the $\mathbf{S}_i$'s being the spin operators at sites i. A numerical expression based on a method developed by Bonner and Fisher[18] has been derived for the molar susceptibility when the interaction is antiferromagnetic:[19]

$$\chi_M = \frac{Ng^2\beta^2}{kT} \frac{0.25 + 0.074\,975x + 0.0752\,35x^2}{1.0 + 0.9931x + 0.1721\,35x^2 + 0.757\,825x^3}$$

with $x = |J|/kT$, g being the Zeeman factor, and the other parameters having their usual meanings. The best fitting in the temperature range 10−300 K is obtained with $J = -28$ cm^{-1} and $g = 2.06$ with a fairly good agreement with experiment. In the crystal the chains of donors are well-isolated from each other, and no interchain interactions take place.

At room temperature $\chi_M T$ of **1a** is equal to 2.25 emu K mol^{-1} in agreement with the expected spin-only value. On cooling to 2 K, $\chi_M T$ decreases (see Figure 14), but contrary to **2b**, no magnetic phase transition occurs at low temperature. One anion can interact with two other anions through the $\pi-\pi$ overlap of isoq groups and also two donor dimers through short S···S contacts. To isolate the chromium contribution to the overall magnetism we subtracted the experimental $\chi_M T$ versus T data of **3a** from the $\chi_M T$ versus T data of **1a** and obtained the chromium contribution to the magnetism of **1a** (Figure 14). The difference curve is almost completely flat down to 12 K with $\chi_M T \approx 1.86$ emu K mol^{-1} and then decreases. The expected value for one isolated chromium with $g = 2.00$ is equal to 1.875 emu K mol^{-1}. We can conclude that anion−anion and donor−anion interactions are small. The dominant interaction in **1a** is donor−donor. Indeed, Mori and Katsuhara[20] have shown that in a similar compound the coupling constant between two chromium spins is of the order of -0.1 cm^{-1}. Furthermore, from the studies of phase **b** compounds we know that the anion−donor interaction through short identical S···S contacts is also small. The net defined by the superexchange interactions between magnetic centers with the orientation of the magnetic moment of the ground state is schematically represented in Scheme 1: J represent the antiferromagnetic coupling between donors along the b axis, J' is the antiferromagnetic coupling within mixed chains in the $[\bar{1}11]$ direction, and J'' is the antiferromagnetic coupling between anions through $\pi-\pi$ overlap of isoq groups along the b axis. With $|J| \gg |J',J''|$ the ground state is antiferromagnetic whatever the ratio J'/J'', and the system can be described, in a first approximation, by two uncoupled magnetic chains: one chain of donors running along the b axis and one chain of anions running also along the b axis. As a matter of fact, the difference curve on Figure 14 can be reproduced with a classical-spin chain model with antiferromagnetic

(17) Kahn, O. *Molecular Magnetism*; VCH: New York, 1993.
(18) Bonner, J. C.; Fisher, M. E. *Phys. Rev. A* **1964**, *135*, 640.
(19) Estes, W. E.; Gavel, D. P.; Hatfield, W. E.; Hogdson, D. *Inorg. Chem.* **1978**, *17*, 1415.
(20) Mori, T.; Katsuhara, M. *J. Phys. Soc. Jpn.* **2003**, *72*, 149.

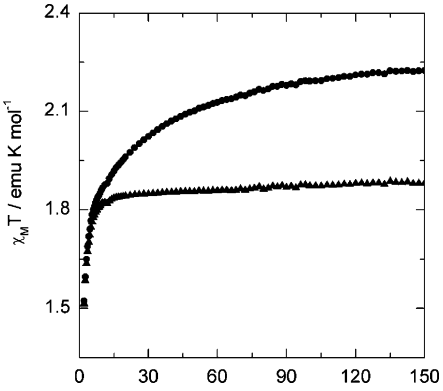

Figure 14. $\chi_M T$ vs T plot for **1a** (●). Chromium contribution ($\chi_M T$(Cr) = $\chi_M T$(**1a**) − $\chi_M T$(**3a**)) (▲).

Scheme 1. Interactions between Spin Carriers[a] in Phase a Compounds with the Relative Orientation of the Spins of the Ground State

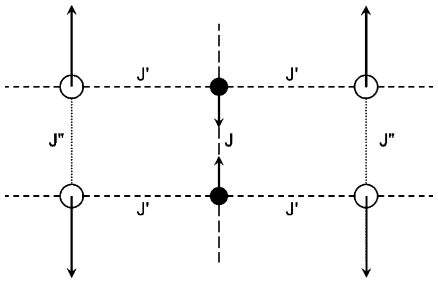

[a] ○, donor dimer; ●, anion.

interaction between neighboring Cr^{III} of the order of −0.1 cm^{-1}. One must also point out that small but significant magnetic anisotropy of distorted octahedral Cr^{III} can contribute to the magnetism.

In phase **a**, the donors form chains which should favor the delocalization of the conducting electrons along the chains. However, these chains are very weakly coupled with the inorganic network. The two networks behave independently with no synergy between them. The delocalization of the spins of the donor, mainly located on the four central sulfur atoms (see Table 8), toward the iodine atoms is too weak to promote superexchange interactions with the inorganic network. The same considerations apply for phase **b**, with, furthermore, no interaction between donors.

Conclusion

We have reported in this article the synthesis and the characterizations of seven charge-transfer salts containing $[M(isoq)_2(NCS)_4]^-$ anions and iodine substituted TTF derivatives. We observed in these compounds a common structural topology. The two iodine atoms of a given TTF donor are connected to two sulfur atoms belonging to the same anion with −I···S− mean distances of 3.4 Å, which is very short compared to the corresponding sum of the vdW radii (3.8 Å). This reflects the ability of iodine to structure materials. The strongly dimerized character of TTFs confers the semiconducting behavior to these compounds. The analysis of the magnetic properties in relation with both their crystal structures and spin density DFT calculations revealed that the very short −I(donor)···S(NCS)− contacts are very efficient for supramolecular self-assembling but not sufficient to mediate significant magnetic interactions between the TTF and the anion. Our analyses reveal also that the main sources of magnetic interactions in our charge-transfer salts are the short S···S intermolecular contacts.

Acknowledgment. This work is supported by the CNRS-JSPS PICS Program No. 1433. K.C. and J.-F.H. thank the Pôle de Calcul Intensif de l'Ouest (PCIO) of the University of Rennes 1 for computing facilities, as well as Dr. S. Kahlal for technical assistance.

Supporting Information Available: Crystallographic data (CIF). This material is available free of charge via the Internet at http://pubs.acs.org.

CM052199Q